AIP | APL Materials

Defect formation in graphene during low-energy ion bombardment

P. Ahlberg, F. O. L. Johansson, Z.-B. Zhang, U. Jansson, S.-L. Zhang, A. Lindblad, and T. Nyberg

Citation: APL Mater. **4**, 046104 (2016); doi: 10.1063/1.4945587
View online: http://dx.doi.org/10.1063/1.4945587
View Table of Contents: http://scitation.aip.org/content/aip/journal/aplmater/4/4?ver=pdfcov
Published by the AIP Publishing

Defect formation in graphene during low-energy ion bombardment

P. Ahlberg,[1] F. O. L. Johansson,[2] Z.-B. Zhang,[1] U. Jansson,[3] S.-L. Zhang,[1] A. Lindblad,[2] and T. Nyberg[1,a]

[1]*Division of Solid-State Electronics, The Ångström Laboratory, Uppsala University, Box 534, SE-751 21 Uppsala, Sweden*
[2]*Department of Physics and Astronomy, Molecular and Condensed Matter Physics, Uppsala University, Box 516, SE-751 20 Uppsala, Sweden*
[3]*Department of Chemistry, Inorganic Chemistry, Uppsala University, Box 538, SE-751 21 Uppsala, Sweden*

(Received 4 February 2016; accepted 23 March 2016; published online 12 April 2016)

This letter reports on a systematic investigation of sputter induced damage in graphene caused by low energy Ar^+ ion bombardment. The integral numbers of ions per area (dose) as well as their energies are varied in the range of a few eV's up to 200 eV. The defects in the graphene are correlated to the dose/energy and different mechanisms for the defect formation are presented. The energetic bombardment associated with the conventional sputter deposition process is typically in the investigated energy range. However, during sputter deposition on graphene, the energetic particle bombardment potentially disrupts the crystallinity and consequently deteriorates its properties. One purpose with the present study is therefore to demonstrate the limits and possibilities with sputter deposition of thin films on graphene and to identify energy levels necessary to obtain defect free graphene during the sputter deposition process. Another purpose is to disclose the fundamental mechanisms responsible for defect formation in graphene for the studied energy range.
[http://dx.doi.org/10.1063/1.4945587]

Since it was first successfully isolated from a graphite crystal over a decade ago, graphene has made it into the laboratories for the development of future generation electronic products.[1,2] Its extreme attributes related to mobility,[3] transparency,[4] and tensile strength[5] make it a suitable material for future electronics. These special properties come from the fact that graphene is a two-dimensional (2D) single layer crystal with delocalized π-electrons organized in a hexagonal network of sp^2 hybridized carbon. However, its 2D geometry is not only an advantage but also poses some challenges, especially when it comes to processing. By definition a single layer 2D material possesses no redundancy of material, meaning that it is inherently sensitive to defects. Several of the current tools used in the production of today's electronics have been utilized in the manufacturing of single layer graphene (SLG) devices. Unfortunately sputter deposition techniques have so far been proven to be incompatible with graphene due to high impact energy of particles, which destroy the sp^2-network of graphene.[6–9] Sputtering is one of the key processes required to incorporate graphene as a component into large-scale manufacturing. Despite this obvious need for knowledge of the limits of sputtering in graphene processing, research here is scarce and is mostly performed by simulations.[10] Here we present an experimental investigation of processing conditions that lead to defect free or close to defect free, sputtering on graphene. We also investigate the dose dependency of defects at certain sputtering energies, aiming at establishing guidelines for optimization of sputter

[a]Author to whom correspondence should be addressed. Electronic mail: Tomas.Nyberg@angstrom.uu.se

deposition processes on graphene. To study only the kinetic aspects of sputtering we restrict ourselves here to Ar ions as projectiles as they are non-reactive. This is in contrast to using, e.g., O which has been shown to react strongly with graphene in its atomic state regardless of the kinetic energy level.[11]

Graphene was in the early studies acquired by mechanical cleavage and this is still the best way to acquire low defect graphene.[2] Chemical vapor deposition (CVD) processing on the other hand is one of the best manufacturing methods for large scale production and is therefore the subject of the study here. It is however associated with problems such as limited grain sizes and defects at the grain boundaries. These defects are reported to be on the nm scale whereas the crystal size in this letter is ~10 μm in size.[12]

The graphene was produced by means of CVD on Cu foils. Feed gases were Ar:H_2:CH_4, 100:75:10 standard cubic centimeter per minute (sccm), respectively. The deposition was carried out at 1000 °C and 187 Pa in a diffusion furnace. Our previously reported residue free transfer method was utilized in order to achieve a clean graphene surface on top of a 300 nm thick SiO_2 surface.[13] Following the transfer, the samples were placed in a vacuum chamber at a pressure of 1.3×10^{-6} Pa where the subsequent ion bombardment took place. The samples were spaced at least 8 cm from each other to prevent stray ions from the Ar^+ beam affecting the neighboring samples. One piece of graphene was used per collected data point. The ion incidence angle was 45° with respect to the substrate.

A Faraday cup was utilized to measure the ion current of the sputter gun for different energies. From this a series of conditions having a constant dose with different Ar^+ kinetic energies could be compiled. Several series with set energies (1, 5, 10, 15, 20, 25, and 40 eV) with different doses were also made. The ion bombarded graphene was subsequently characterized by means of resonant Raman spectroscopy at 532 nm wavelength and 20× magnification in a Renishaw "inVia" Raman Spectrometer.

We use Raman spectroscopy for damage assessment of graphene irradiated with Ar^+. Models evaluating the quality and behavior of graphene from Raman spectroscopy have been made available during the last years.[14–18] The Raman spectrum of graphene has three distinct peaks that can be used to examine the quality of a graphene specimen: the D, G, and 2D peaks at 1350, 1580, and 2700 cm^{-1} respectively, see Fig. 1(a). Throughout this paper, peak intensity is taken to be equivalent to a peak's height. The G peak is present due to an in-plane vibrational mode not affected by defects and is therefore used as the standard level for normalizing spectra.[16] The D peak only activates in

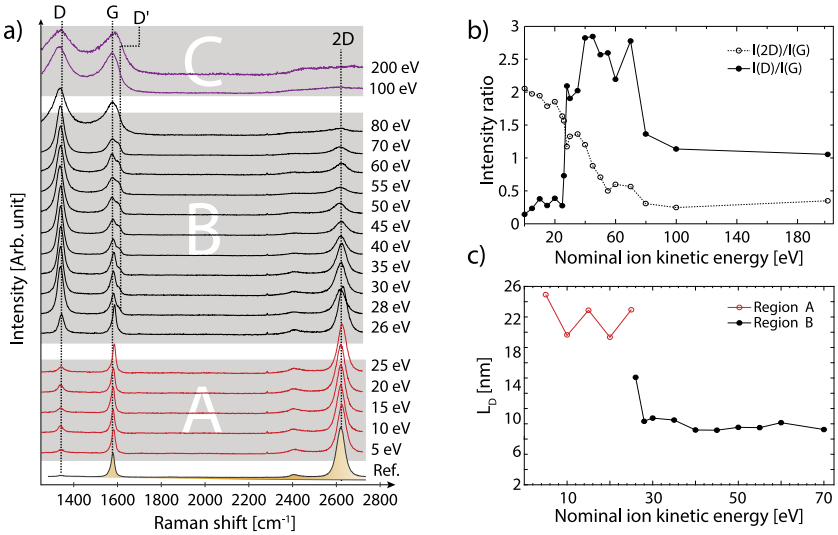

FIG. 1. (a) Raman spectra of graphene exposed to same Ar^+ ion dose but at different ion energies. (b) Intensity ratios of 2D to G and D to G Raman peaks vs. kinetic energy of the ions bombarding the graphene sample seen in (a). (c) L_D calculated from the I(D)/I(G) and I(2D)/I(G) ratios seen in (b).

the presence of defects, it is therefore directly correlated to the amount of defects in the graphene film.[16] This is in contrast to the 2D peak that accounts for the amount of carbon in graphene with no defects in its proximity.[16] In the discussion that follows a fourth peak (D′) will also be of interest: the D′ peak is located at slightly higher shift than the G peak and also requires a defect to become activated.[14]

In the reference curve (bottom curve Fig. 1(a)) of freshly transferred SLG the 2D peak at 2700 cm^{-1} and the G peak at 1590 cm^{-1} can clearly be seen. Also present but less obvious is the D peak at 1380 cm^{-1}. When increasing the ion energy, we can see in Fig. 1 that the 2D peak decreases while the D peak increases and the G peak retains its intensity. It can be noted that a second peak appears at 1600 cm^{-1} from ion energies at 28 eV and upwards. The peak with the lower Raman shift of the two is the one being referred to as the G peak, whereas the one at the higher shift is the D′ peak. Additional samples of different dosages and energies were also collected. These follow the same development.

From Fig. 1, it is possible to distinguish three regions of effect: A, B, and C. Region A refers to kinetic energies below 26 eV, here no damage seem to occur at the tested dose of 3×10^{14} ions/mm^2. Region B, with energies between 28 and 80 eV, has similar defect levels throughout the series. Furthermore, it is here the D′ peaks are the most pronounced. In region C, above 80 eV, the damage is so extensive that the graphene is indistinguishable from amorphous carbon. The intensity of the 2D peak decrease almost linearly until it completely vanishes somewhere below 200 eV. As mentioned above, the 2D peak intensity is directly correlated to the amount of graphene not effected,[19] and it is therefore not surprising that it vanishes at ion energies of 80 eV (Fig. 1(a), region C), as this is the same ion energy that the D and G peaks have broadened in a manner commonly related to amorphization of the graphene. Several publications have shown that the I(D)/I(G) ratio can be used to calculate the mean distance between defects, this model has been proven valid for point defect evaluation in large (≫30 nm) graphene crystals.[14,15] Here we utilize the simplified equation: $I(D)/I(G) = (1.8 \pm 0.5) \times 10^{-9}\lambda^4/L_D^2$, where L_D is the mean distance between defects in a graphene film and λ is the Raman wavelength (532 nm).[14] This equation is used in Fig. 1(c) to estimate the level of induced damage. It is seen that $L_D \approx 22 \pm 2$ nm for the ion energies in the A region, whereas the B region plateaus at about $L_D \approx 7 \pm 15$ nm (see Fig. 1(c)).[14] A D′ peak will be seen when the defects are less than 15 nm from each other.[14] We can see here that this behavior occurs when the intensity ratio of D to G peaks approaches 2. A ratio between 2 and 3 is considered the maximum level for the laser wavelength of 532 nm used here, since then the defects start to merge and the material approaches a structure more and more akin to amorphous carbon.

The displacement energy E_d, i.e., the energy required to remove one carbon atom from a pristine graphene sheet has been calculated to about 22.2 eV.[10,20] For argon (or other) ions, the kinetic energy required by the ion to remove a C atom is found via the kinematical relationship which describes the transfer of kinetic energy from an incoming ion to a target atom,

$$E_{\min} = \frac{E_d(m_c + M)^2}{4m_c M}. \quad (1)$$

Here m_c and M are the C and Ar^+ masses, respectively. The kinetic energy, E_{min}, required for an Ar ion to displace a carbon atom in a suspended graphene sheet is then 31.2 eV.[10] At graphene grain boundaries the enthalpy is positive vis-'a-vis pristine graphene.[21] This suggests that the displacement energy can be lower than 22.2 eV. The presence of a substrate, and the fact that the angle of ion impact to the substrate is 45°, may result in conditions deviating from the ideal situation assumed in the simulations, i.e., a head on impact with the projectile trajectory being perpendicular to a perfectly flat, suspended graphene sheet. It is however still reasonable to expect a lower energy limit of around 30 eV to achieve displacement deformation/sputter removal of perfect graphene.

Fig. 1(b) presents our measured ratios I(D)/I(G) and I(2D)/I(G) plotted vs. ion energy. Around 25 eV there is a clear transition between two different regions. The fact that the measured energy (E_d) is closer to 25 eV than 33 eV could be explained with the energy distribution of the ions generated by the ion gun. In an ion gun system there will normally be a certain level of double ionization of the atoms leading to a substantial amount of double charged ions. This particular

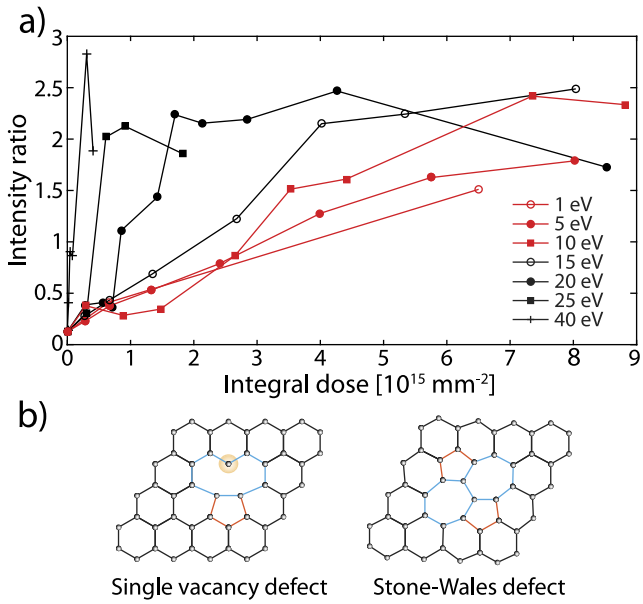

FIG. 2. (a) I(D)/I(G) as a vs. ion dose (exposure time) for different energies illustrating the two separate energy regions, 1-15 eV being the low energy region and 20 and upward being the high energy region, correlating to the two different dominant defect formation mechanisms. (b) Illustrations depicting different types of defects from energetic ion bombardment, displacement defects from high energy impact (left) and isomerization from low energy impact (right).

system has been measured to give a few tens of percent of double ionized Ar (i.e., double kinetic energy) which cannot be ignored.

To investigate the different defect formation mechanisms at different ion energies, a study of the induced damage vs. ion dose at different ion energies was conducted. Fig. 2(a) shows I(D)/I(G) vs ion dose for different energies. Even if the kinetic energy of the ions is below 25 eV, we see that a prolonged exposure can still affect the graphene at energies as low as a few eV (considering the double ionization of the 1 eV ions). Simulations have shown that bond breaking should not arise with energies below 20-33 eV.[10] In contrast, our experiments show that defects are generated at the lowest energy considered here: 1-2 eV. There is, for example, so called Stone-Wales (SW) defects which have shown to occur at energy levels around 10 eV.[22] This type of defect comes from an isomerization of the carbon atoms, turning four hexagonal rings in graphene into two heptagonal and two pentagonal ones, see Fig. 2(b) (right illustration). Since no bonds are broken, but merely rearranged, the energy to obtain this change can be very low. Although the SW defects have not been reported at such low energies, it can be assumed that it may occur due to multiple simultaneous impact or other low probability mechanisms. There are different defects present in a pristine graphene film produced by CVD. These defects are primarily located at grain boundaries and introduce strain in the film which will affect how the graphene react to ionic bombardment. These defects arise during the CVD growth when two graphene crystals coalesce, whereby heptagonal and pentagonal rings are formed to compensate for the crystal misalignment. Some of these defective bonds have been calculated to have binding energies close to 1 eV making them susceptible to damage by ionic impact.[22]

In Fig. 2(a) it is possible to distinguish two separate dynamic behaviors; for energies from 15 eV and below, the defect formation rate is rather constant and significantly lower than for the energies at 20 eV and above. The significant amount of double ionized Ar implies a substantial amount of 40 eV ions in the 20 eV beam, which is well above the energy threshold for obtaining amorphous graphene; see Fig. 2(b) (left illustration). The same is true for higher energies, i.e., 25 and 40 eV. The fact that the breaking point in Fig. 1 was concluded to be 25 eV is explained by the low dosage insufficient to deliver a measurable amount of double ionized ions of 50 eV. The defects of the lower energies become measureable around an integral dose of 7×10^{14} ions/mm^2.

This refers to a situation where either the graphene crystals have shrunk to the size of around 30 nm in size or there are point defects in the graphene separated by roughly the same average distance.[14,15] Given the low bond energy is calculated for carbon at the graphene crystal boundaries, there is a possibility for low energetic ions to damage the crystal from the edge and inwards. If the responsible mechanism is the destruction starting at the grain boundaries between coalesced crystal islands and moving inwards from the edges, the crystalline part of the graphene would shrink from 10 μm to 30 nm from an ion dose of 7×10^{14} ions/mm^2 while it would take up to a ten times higher dosage to shrink from 30 to 5 nm.[14] As this is highly unlikely, an introduction of spot wise defects, see Fig. 2(b) (left illustration), is concluded to be the most dominating mechanism. By calculating L_D from the data acquired for the 15 eV series, according to the previously mentioned model see Fig. 2(a),[14] we can estimate that, on average, 22 ions are required to introduce one defect. The results presented in Fig. 2(a) are useful when designing a process for sputtering onto graphene without introducing defects if energy distribution and flux during the deposition can be estimated. For example, if it is known that the maximum energy is less than 30 eV, one has to deposit a pinhole free film, protecting the graphene from ion radiation, before the integral dosage reaches 1×10^{15} mm^{-2}.

In conclusion, we have demonstrated that graphene can be damaged by Ar^+ ions having nominal energies in the few eV region. There are primarily two different defect formation mechanisms depending on energy. At energies below 30 eV the responsible mechanism for defect formation is isomerization and at higher energies the dominant mechanism is creation of displacement defects/sputtering. However, due to the significant amount of double ionized Ar displacement defects are observed at ion energies as low as 20 eV. The clear trend of increasing I(D)/I(G) vs. both dose and kinetic energy shows that sputter deposition on graphene is possible but challenging. If the flux and energy distribution of species arriving at the graphene substrate is known in a sputter deposition process, the presented results may be used as guidelines to tailor make a process for sputtering onto defect free graphene. Thus a relation between the required sputter deposition rate and energy/flux can be derived from results presented herein.

This work was financially supported in part by the Knut and Alice Wallenberg Foundation (No. 2011.0082), the Swedish Research Council (Nos. 2014-5591 and 2014-6463) and Marie Sklodowska Curie Actions, Cofund, Project INCA 600398.

[1] A. C. Ferrari, F. Bonaccorso, V. Falko, K. S. Novoselov, S. Roche, P. Boggild, S. Borini, F. Koppens, V. Palermo, N. Pugno, J. A. Garrido, R. Sordan, A. Bianco, L. Ballerini, M. Prato, E. Lidorikis, J. Kivioja, C. Marinelli, T. Ryhanen, A. Morpurgo, J. N. Coleman, V. Nicolosi, L. Colombo, A. Fert, M. Garcia-Hernandez, A. Bachtold, G. F. Schneider, F. Guinea, C. Dekker, M. Barbone, C. Galiotis, A. Grigorenko, G. Konstantatos, A. Kis, M. Katsnelson, C. W. J. Beenakker, L. Vandersypen, A. Loiseau, V. Morandi, D. Neumaier, E. Treossi, V. Pellegrini, M. Polini, A. Tredicucci, G. M. Williams, B. H. Hong, J. H. Ahn, J. M. Kim, H. Zirath, B. J. van Wees, H. van der Zant, L. Occhipinti, A. Di Matteo, I. A. Kinloch, T. Seyller, E. Quesnel, X. Feng, K. Teo, N. Rupesinghe, P. Hakonen, S. R. T. Neil, Q. Tannock, T. Lofwander, and J. Kinaret, Nanoscale **7**, 4598 (2014).

[2] K. S. Novoselov, A. K. Geim, S. V. Morozov, D. Jiang, Y. Zhang, S. V. Dubonos, I. V. Grigorieva, and A. A. Firsov, Science **306**(5696), 666 (2004).

[3] K. I. Bolotin, K. J. Sikes, Z. Jiang, M. Klima, G. Fudenberg, J. Hone, P. Kim, and H. L. Stormer, Solid State Commun. **146**(9-10), 351 (2008).

[4] R. R. Nair, P. Blake, A. N. Grigorenko, K. S. Novoselov, T. J. Booth, T. Stauber, N. M. R. Peres, and A. K. Geim, Science **320**(5881), 1308 (2008).

[5] C. Lee, X. Wei, J. W. Kysar, and J. Hone, Science **321**(5887), 385 (2008).

[6] O. Lehtinen, J. Kotakoski, A. V. Krasheninnikov, and J. Keinonen, Nanotechnology **22**(17), 175306 (2011).

[7] C.-T. Chen, E. A. Casu, M. Gajek, and S. Raoux, Appl. Phys. Lett. **103**(3), 033109 (2013).

[8] X. P. Qiu, Y. J. Shin, J. Niu, N. Kulothungasagaran, G. Kalon, C. Qiu, T. Yu, and H. Yang, AIP Adv. **2**(3), 032121 (2012).

[9] G. Compagnini, F. Giannazzo, S. Sonde, V. Raineri, and E. Rimini, Carbon **47**(14), 3201 (2009).

[10] O. Lehtinen, J. Kotakoski, A. V. Krasheninnikov, A. Tolvanen, K. Nordlund, and J. Keinonen, Phys. Rev. B **81**(15), 153401 (2010).

[11] N. A. Vinogradov, K. Schulte, M. L. Ng, A. Mikkelsen, E. Lundgren, N. Mårtensson, and A. B. Preobrajenski, J. Phys. Chem. C **115**(19), 9568 (2011).

[12] P. Y. Huang, C. S. Ruiz-Vargas, A. M. van der Zande, W. S. Whitney, M. P. Levendorf, J. W. Kevek, S. Garg, J. S. Alden, C. J. Hustedt, Y. Zhu, J. Park, P. L. McEuen, and D. A. Muller, Nature **469**(7330), 389 (2011).

[13] M. Hinnemo, P. Ahlberg, C. Hägglund, W. Ren, H.-M. Cheng, S.-L. Zhang, and Z.-B. Zhang, Carbon **98**, 567 (2016).

[14] L. G. Cançado, A. Jorio, E. H. Martins Ferreira, F. Stavale, C. A. Achete, R. B. Capaz, M. V. O. Moutinho, A. Lombardo, T. S. Kulmala, and A. C. Ferrari, Nano Lett. **11**(8), 3190 (2011).

[15] M. M. Lucchese, F. Stavale, E. H. Martins Ferreira, C. Vilani, M. V. O. Moutinho, R. B. Capaz, C. A. Achete, and A. Jorio, Carbon **48**(5), 1592 (2010).
[16] A. C. Ferrari and D. M. Basko, Nat. Nanotechnol. **8**(4), 235 (2013).
[17] A. C. Ferrari and J. Robertson, Phys. Rev. B **61**(20), 14095 (2000).
[18] A. C. Ferrari and J. Robertson, Phys. Rev. B **64**(7), 075414 (2001).
[19] J. Ado, M. Lucchese Marcia, S. Fernando, H. Martins Ferreira Erlon, V. O. Moutinho Marcus, B. Capaz Rodrigo, and A. Achete Carlos, J. Phys.: Condens. Matter **22**(33), 334204 (2010).
[20] A. Merrill, C. D. Cress, J. E. Rossi, N. D. Cox, and B. J. Landi, Phys. Rev. B **92**(7), 075404 (2015).
[21] C. Ophus, A. Shekhawat, H. Rasool, and A. Zettl, Phys. Rev. B **92**(20), 205402 (2015).
[22] F. Banhart, J. Kotakoski, and A. V. Krasheninnikov, ACS Nano **5**(1), 26 (2011).